

Application of scientific visualization tools in the study of supersonic vortex pair

V.E. Borisov¹, A.A. Davydov², T.V. Konstantinovskaya³, A.E. Lutsky⁴

Keldysh Institute of Applied Mathematics RAS

¹ ORCID: 0000-0003-4448-7474, narelen@gmail.com

² ORCID: 0000-0001-5662-817X, ryzhiy@list.ru

³ ORCID: 0000-0002-1127-503X, konstantinovskaya.t.v@gmail.com

⁴ ORCID: 0000-0002-4442-0571, allutsky@yandex.ru

Abstract

Scientific visualization is an important stage of research. It is intended to provide post-processing analysis tools for presenting the results obtained numerically and/or experimentally. This is especially topical with regard to the increasing volume of processed data associated with the productive capacity growth of computing systems.

In this work two scientific visualization methods were applied to recognize flow parameters obtained by numerical simulation of counter-rotating supersonic vortex pair interaction: the λ_2 -method and maximum vorticity method.

The results of their application are compared. The numerical data was obtained by a computational model based on the URANS equations with SA turbulence model. Numerical simulations were performed on the hybrid supercomputing system K-60 at the Keldysh Institute of Applied Mathematics RAS. The main simulation results are presented and analyzed.

Keywords: supersonic flow, vortex flow, counter-rotating pair, scientific visualization.

1. Introduction

Vortex flows are ubiquitous both in natural phenomena and in technological processes. When studying a particular type of flow, it is very important to identify/determine the main constitutive structural elements of a sufficiently large scale. For example, such elements as a shock wave, a rarefaction wave, a separation region, a vortex, and so on. And for this purpose, visualization tools are well suited: they provide analysis tools that help to study the structure of the flow, to determine its features and main characteristics.

Scientific visualization is used in many fields. There are many approaches to describing data using its methods [1]. For example, regarding the visualization of vortex flows, large reviews of the used methods are made [2-5]. The main methods used for visualization of vortex flows are described, and their comparative analysis is carried out in these works. The most commonly used methods in this area are: λ_2 -method, Q-method, vorticity calculation, etc. The authors here only mention some of the visualization methods, without setting the goal of their detailed study and description.

The authors did not set the problem of visualization methods comparison, but investigated an important problem of aerodynamics - the problem of propagation of supersonic tip vortices, in particular, pairs of wingtip vortices in counter-rotating configuration. This task is particularly topical in view of the increased interest in supersonic aircraft both in civil aviation and in military industry. A vortex wake that appears behind any aircraft carries a potential hazard to the following aircraft [6]. In addition, especially in the case of supersonic modes, there is a risk of getting a vortex trace on other elements of the aircraft located downstream, in particular, in the combustion chamber of propulsion system [7]. This can lead to a change in the lift

force, additional overloads on the aircraft body, as well as to engine outages. At the same time, such flows as a vortex wake behind a blunt body can be considered from the point of view of coherent structures [8, 9], which makes it possible to further expand the tools for analyzing such vortex flow data and consider them from a different point of view.

Up till now, there is no unambiguous universally accepted definition of a vortex [5, 10, 11]. The vortex intuitively is characterized by the rotational movement of the material particles around the central region. However, it is difficult to put this understanding in the strict framework of a clear formal definition.

Scientific visualization methods allowed the authors to illustrate the main properties of the studied flow based on the obtained information, in particular, to determine the axis of supersonic wingtip vortices. In addition, it was shown that different visualization methods can complement each other well, giving an idea of the studied flow from different sides and reflecting its main properties and structures. The authors have already appealed to visualization methods [12], but now they continue to deepen and expand the application of scientific visualization methods to new problems with an ever-growing volume of data.

This paper demonstrates the application of scientific visualization methods to the problem of a pair of streamwise supersonic counter-rotating wingtip vortices propagation at the incoming flow Mach number $M_\infty = 3$.

2. Problem Statement

The flow behind two coaxial wings with sharp leading, trailing, and side edges and with a diamond-shaped base was studied numerically (fig.1). The wings were located at an angle of 10° to the incoming flow and were attached to the walls parallel to flow direction with the base. The simulations were performed in dimensionless variables [13], a unit of length was taken $L = 1$ m. Density and pressure were non-dimensionalized by its free stream values. The chord of each wing was equal to $b = 0.03$, half-span of first wing was $l_1 = 0.075$, the second one was $l_2 = 0.095$. The thickness of the diamond-shaped base of both wings was equal to $h = 0.004$. The distance between the tip chords of the wings was $l_3 = 0.03$, so the width of the area between the walls was $H = 0.2$. The x axis was co-directed to the incoming flow. The z axis coincided with the common axis of the wings. The y axis was directed from the leeward side of the wings to the windward side. The length of the area under consideration was up to 10 wing chords downstream from the common axis of the wings. The Reynolds number in simulation was $Re_L = 1 \times 10^7$.

3. Numerical Model

The numerical simulation was performed on 224 computational cores of the hybrid supercomputing system K-60 [14] at the Keldysh Institute of Applied Mathematics RAS using the developed software package. A system of URANS equations with SA turbulence model for compressible flows [15] with Edwards modification [16] was used for describing a supersonic flow of a perfect viscous compressible fluid. The finite volume method based on the reconstruction schemas of the second order (TVD) was used. Time approximation was performed by means of an explicit scheme. A more detailed description of the numerical algorithms is given [17]. Simulations were carried out on an unstructured mesh with 25 774 200 hexagonal cells. The mesh was refined in the zones of vortex formation and its propagation throughout overall simulation domain for better resolution of vortex structures.

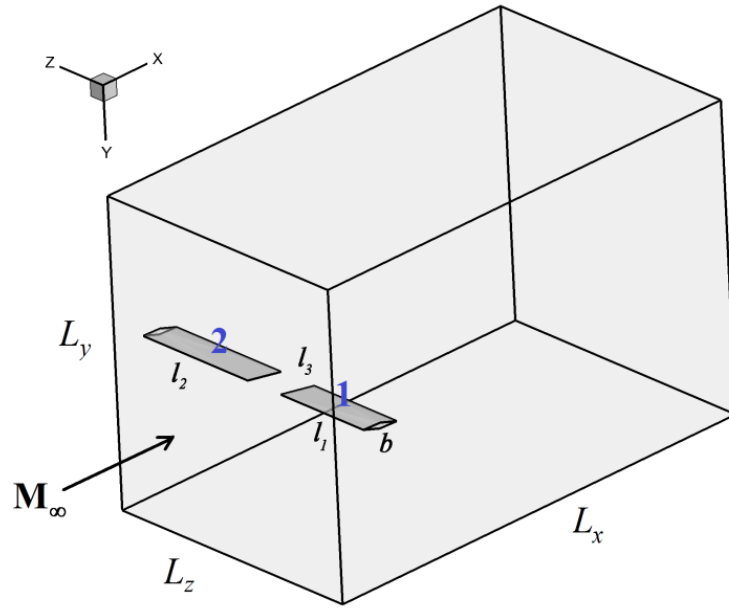


Figure 1. General model scheme

4. Vortex Visualization

A separate post-processing data simulation module was developed for determining vortex structures for hexagonal grids within the developed software package. The maximum vorticity method is fully implemented in it, and the necessary matrices are calculated for applying the λ_2 -method. The module generates data of vortex structures in the format of the Tecplot software package, which is used for further visualization of numerical simulation results.

4.1. λ_2 -method

The λ_2 -method (or criterion) for identification of vortices was proposed [18]. According to this criterion, the vortex flow region is determined based on the analysis of the eigenvalues of the symmetric matrix $\mathbf{A} = \mathbf{S}^2 + \mathbf{\Omega}^2$, which are always real (here \mathbf{S} and $\mathbf{\Omega}$ are the strain-rate and vorticity tensors of the flow respectively):

$$\nabla \mathbf{u} = \mathbf{S} + \mathbf{\Omega}, \quad S_{i,j} = \frac{1}{2} \left(\frac{\partial u_i}{\partial x_j} + \frac{\partial u_j}{\partial x_i} \right), \quad \Omega_{i,j} = \frac{1}{2} \left(\frac{\partial u_i}{\partial x_j} - \frac{\partial u_j}{\partial x_i} \right),$$

where $\nabla \mathbf{u}$ is velocity gradient tensor.

According to this method, the vortex region is considered to be the part of space in which the second eigenvalue $\lambda_2(\mathbf{A}) < 0$ ($\lambda_1 \geq \lambda_2 \geq \lambda_3$). This method is quite widespread and is often used in data processing.

4.2. Maximum vorticity method

The maximum vorticity method was proposed in [19]. It is based on one of the definitions of vortex flow and consists in detection the local maximum of the vorticity vector modulus $|\boldsymbol{\omega}| = |\nabla \times \mathbf{u}|$ in the plane perpendicular to the direction of this vector. This method allows to determine the exact axis of the streamwise vortex in the case of sufficient resolution of the computational mesh.

4.3. Application results

If the maximum vorticity method is intuitive enough, then the λ_2 -method is not so obvious. To clear demonstrate the operation of the two mentioned scientific visualization methods, especially the λ_2 -method, the authors applied them to a model problem – to Burger's vortex.

The authors did not set out to investigate the λ_2 -method, but only wanted to test its work on a visual example. The Burger's vortex was chosen as such a visual example. Burger's vortex was taken in cylindrical coordinates as follows [19]:

$$\begin{aligned} V_r &= 0 \\ V_\theta &= \frac{\Gamma_0}{r} \left(1 - \exp \left[- \left(\frac{r}{r_c} \right)^2 \right] \right) \\ V_x &= \text{const} = 3 \end{aligned}$$

where $\Gamma_0 = 0.4$, $r_c = 0.25$.

The application results of two mentioned visualization methods to the Burger's vortex are presented in the figure 2. The iso-surface of $\lambda_2 = 0$ and vortex axis determined by maximum vorticity method are demonstrated in this figure. It can be seen that the λ_2 -method adequately represents and displays the given Burger's vortex. The vortex axis was also found correctly using the maximum vorticity method. Thus, these two methods work adequately on the selected model problem.

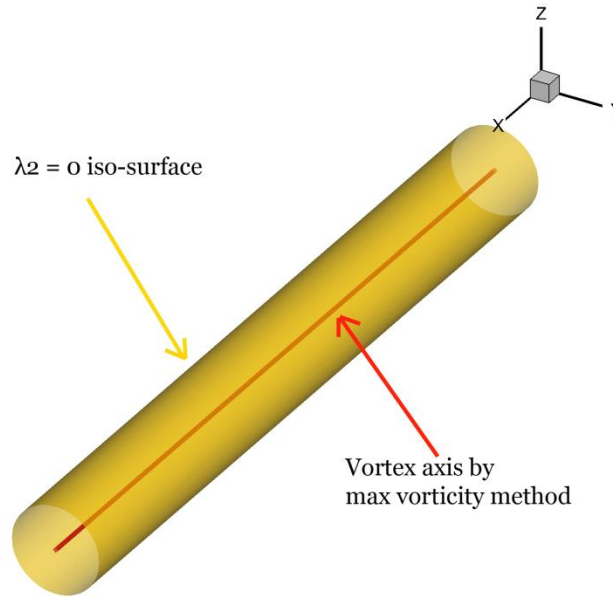


Figure 2. Application of λ_2 and maximum vorticity methods to model problem – Burger's vortex.

Now let's return to the problem of a streamwise counter-rotating supersonic vortices pair propagation (fig. 1). Figure 3 shows the results of the λ_2 -method applying to visualize the simulation results of the described problem. This method allows us to find the vortex flow region bounded by the iso-surfaces of the negative eigenvalue $\lambda_2(\mathbf{A})$.

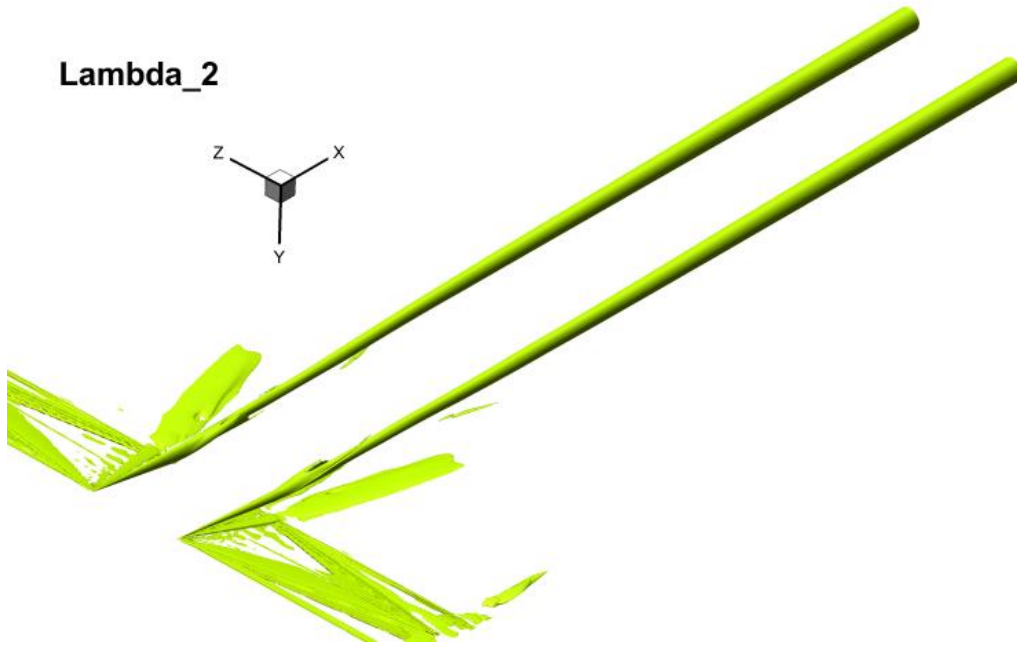


Figure 3. Pair of supersonic counter-rotating wingtip vortices visualized by means of λ_2 -method (iso-surfaces of level $\lambda_2 = -600$).

Figure 4 shows the iso-surfaces of the level $\lambda_2 = -600$ in sections perpendicular to the direction of the incoming flow: $x = 0.1$, $x = 0.2$, $x = 0.3$. In the section $x = 0.1$, the values of λ_2 are shown by filling in red and blue, in the section $x = 0.2$ – by a green circle, in the section $x = 0.3$ – by a black circle. It is noted the displacement of counter-rotating vortices upside (to leeward wing side) and their divergence at considered distances downstream from the wing axis, which correlates with the data of other authors [21, 22]. The diameter of the vortex zone expands downstream from the wing axis, forming a cone-like shape of the vortices.

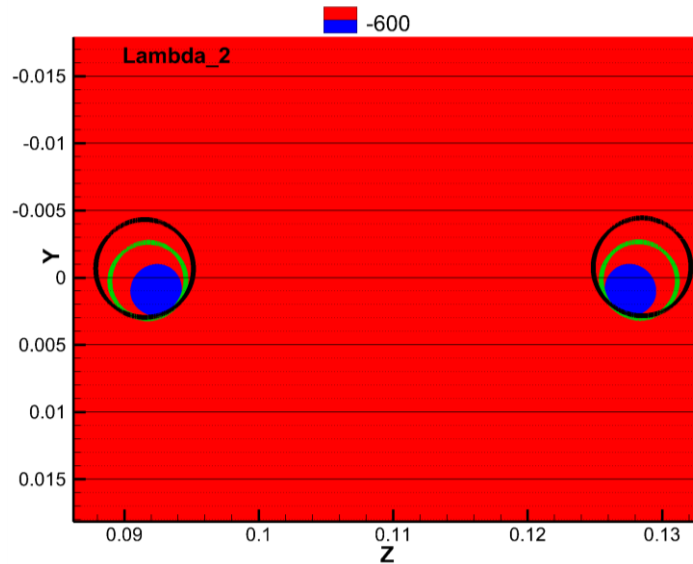


Figure 4. Iso-surfaces of level $\lambda_2 = -600$ in cross-section $x = 0.1$ (filling in red and blue separation), $x = 0.2$ (green circle), $x = 0.3$ (black circle).

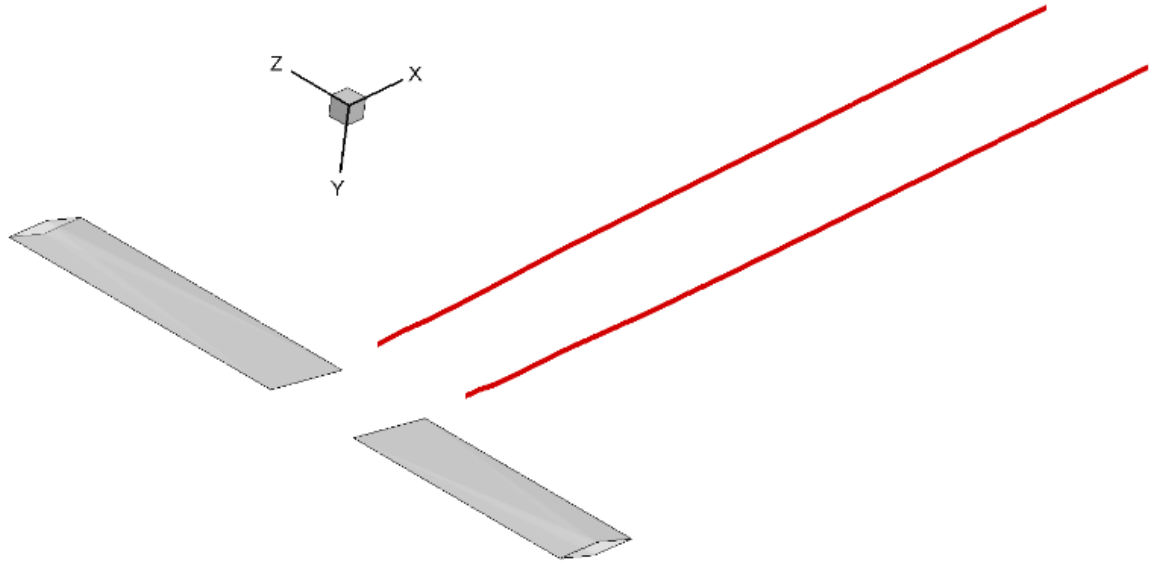


Figure 5. Axes of supersonic counter-rotating wingtip vortices pair (red lines) determined by the maximum vorticity method.

Figure 5 shows the axes of the wingtip vortices that are found by the maximum vorticity method for the problem under investigation (red lines). This allows us to plot the coordinates of the vortex axes y and S (the distance between the vortex axis coordinate z and the tip chord of the corresponding wing-generator) which are shown in figure 6. As mentioned above, it is noted the displacement of the vortex axes upward (to leeward wing side), as well as their repulsion from each other. There is a section of non-monotonicity on the graphs of the vortex axes coordinates at the near wing region at small values of x about $x = 0.05 \dots 0.09$, which is associated, firstly, with the zone of vortex formation, and, secondly, with the arrival of a weak compression wave from the edge of the neighboring wing.

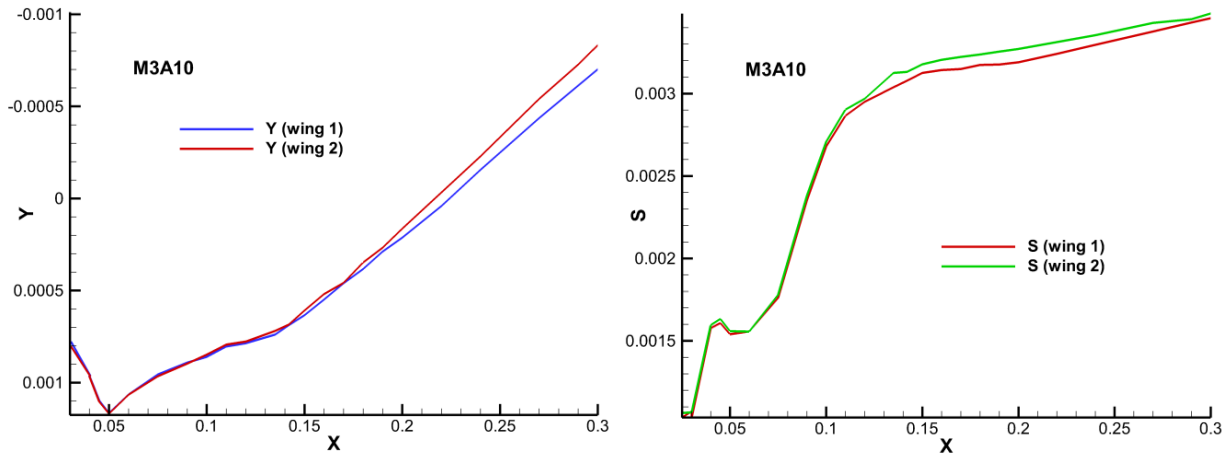


Figure 6. Axis coordinates of counter-rotating vortices: y (left) and S (right).

The visualization of the vortex formation region (the zone of the vortex rope formation) is of particular interest, a more detailed conception of which can be obtained by the vorticity iso-surfaces. For example, fig. 7 shows how the veil from the tip edge of the wing is folded into a rope. However, in our previous works, we were interested in long distance region, and the near region remained little studied in our researches. This will be the topic of further research.

Figure 8 shows both the position of the axes of a counter-rotating vortex pair identified by the maximum vorticity method (red lines) in the region of the formed vortex and the vortex core identified by the λ_2 -method (green iso-surfaces), $\lambda_2 = -600$.

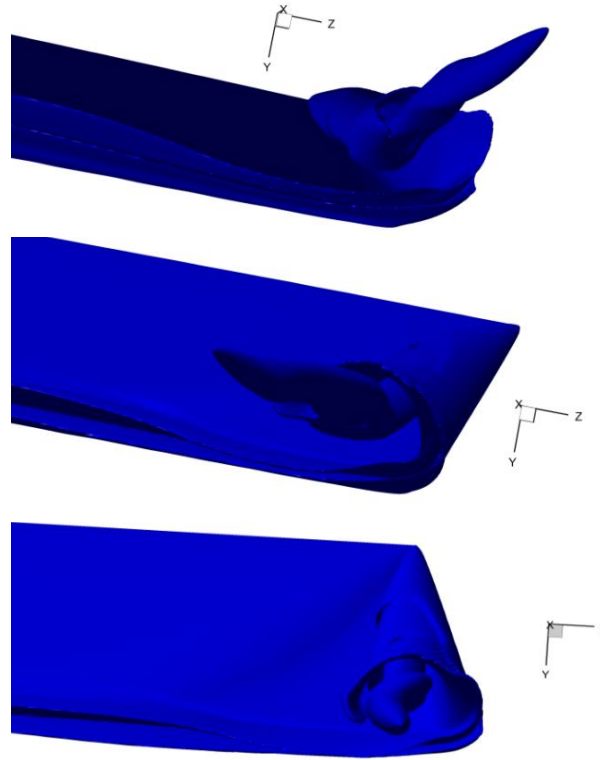


Figure 7. Zone of vortex rope formation: vortex iso-surfaces of level 2000 for the wing with a half-span of 0.075 at different angles of view.

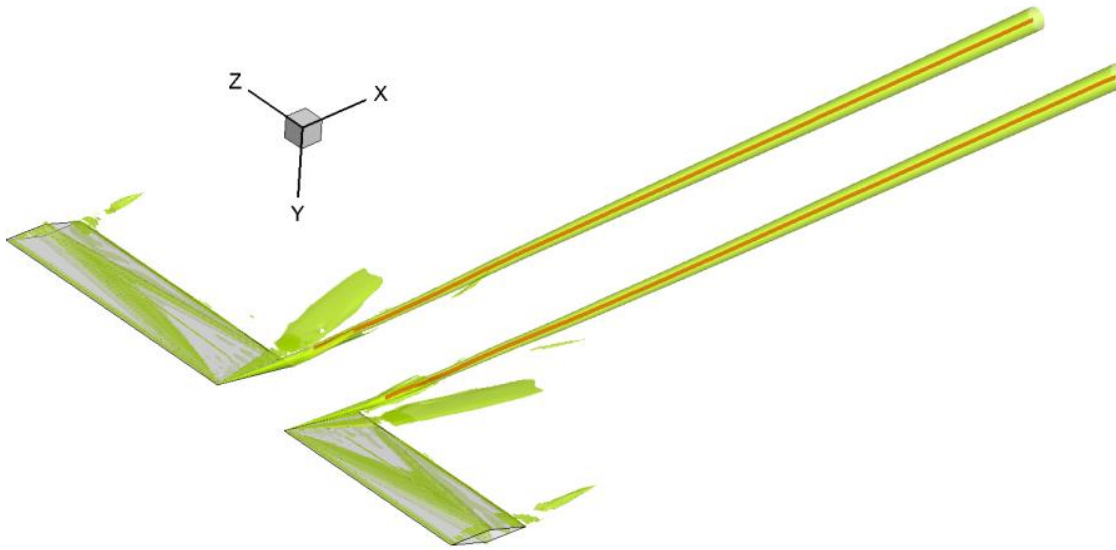


Figure 8. Superposition of vortex axes (red lines) identified by maximum vorticity method and of vortex cores identified by the λ_2 -method, $\lambda_2 = -600$.

These two visualization methods give the results that are well compatible with each other. Moreover, they complement each other, giving a more detailed idea of the main properties and structures of a counter-rotating vortex pair.

5. Conclusion

In this paper we demonstrate the employment of scientific visualization tools in the study of supersonic counter-rotating vortex pair. Two visualization methods have been applied to numerical data obtained on the supercomputer system K-60: λ_2 -method and maximum vorticity method.

They give well consistent results: the λ_2 -method provides a visual representation of the vortex core, while maximum vorticity method allows to find the vortex axis. In addition, the vorticity iso-surfaces provide an opportunity to demonstrate clearly how the vortex rope curls up in a formation zone. Moreover, used two visualization methods complement each other, showing different aspects of the considered flow, which can be used in the future to analyze processes in the vortex zone.

In general, it can be noted that scientific visualization methods allow to get a main structures and certain details of the investigated flow what gives an major asset in the scientific research.

References

1. Hansen C.D., Johnson C.R. (Eds.). *The Visualization Handbook*. NY: Academic Press, 2004, 984 p.
2. Chakraborty, P., Balachandar, S., Adrian, R. G. On the relationships between local vortex identification schemes. *J. Fluid Mech.*, **535**, pp 189-214, 2005.
3. Kolář V. Brief Notes on Vortex Identification. *Recent Advances in Fluid Mechanics, Heat and Mass Transfer and Biology* (WSEAS Press, 163 p), pp 23-29, 2011.
4. Volkov K.N. Visualization methods of vertical flows in computational fluid dynamics and their applications. *Scientific and Technical Journal of Information Technologies, Mechanics and Optics*, **91** 3, 2014 (in Russian).
5. Volkov K.N., Emelyanov V.N., Teterina I.V., Yakovchuk M.S. Methods and concepts of vortex flow visualization in the problems of computational fluid dynamics. *Num. Methods and Programming*, **17** 1, 2016 (in Russian).
6. Wake Turbulence Training Aid (section 2), FAA Report, United States Department of Transportation.
7. Vergine F., Maddalena L. Study of two supersonic streamwise vortex interactions in a Mach 2.5 flow: Merging and no merging configurations. *Physics of Fluids*, **27**, 076102, 2015.
8. Bock B. Coherent structures in the wake of a SAE squareback vehicle model. arXiv:2008.03783, 2020.
9. Hussain F. Coherent structures and turbulence. *J. Fluid Mech.*, **173**, pp 303-356, 1986.
10. Haller G. An objective definition of a vortex. *J. Fluid Mech.*, **525**, pp 1-26, 2005.
11. Kolář V. Vortex identification: New requirements and limitations. *International Journal of Heat and Fluid Flow*, **28**, pp 638–652, 2007.
12. Konstantinovskaya T., Lutsky A. Numerical simulation and visualization of wing vortices. *Scientific Visualization*, Vol. **4**, №2, pp 14-20, 2012.
13. Bykov L.V., Molchanov A.M., Scherbakov M.A., Yanyshch D.S. *Computational mechanics of continuous media in problems of aviation and space technology*. LENAND, 2019, 668 p (in Russian).
14. www.kiam.ru
15. Allmaras S. R., Johnson F. T., Spalart P. R. Modifications and Clarifications for the Implementation of the Spalart-Allmaras Turbulence Model. *Seventh International Conference on CFD (ICCFD7)*, Big Island, Hawaii (9-13 July 2012).
16. Edwards J. R., Chandra S. Comparison of eddy viscosity-transport turbulence models for three-dimensional, shock-separated flowfields. *AIAA Journal* **34** 4, pp 756–763, 1996.
17. Borisov V. E., Lutsky A. E. Simulation of transition between regular and Mach shock waves reflections by an implicit scheme based on the LU-SGS and BiCGStab methods. *KIAM Preprint* **68** (2016) DOI:10.20948/prepr-2016-68 (in Russian).
18. Jeong J., Hussain F. On the identification of a vortex. *Journal of Fluid Mechanics*, **285**, pp 69–94, 1995.

19. Alekseenko S.V., Kuibin P.A., Okulov V.L. Introduction to theory of concentrated vortices. Institute of Thermophysics, Novosibirsk, 2003, 504 p.
20. Strawn R.C., Kenwright D.N., Ahmad J. Computer visualization of vortex wake systems. *AIAA Journal*, **37** 4, pp 511–512, 1999.
21. Forster K.J., Barber T.J., Diasinos S., Doig, G. Interaction of a counter-rotating vortex pair at multiple offsets. *Experimental Thermal and Fluid Science J.*, **86**, pp 63-74, 2017.
22. Lamb H. Hydrodynamics. Cambridge UK: Cambridge Univ. Press, 6th ed., 1932, 738 p.